Validation of Advanced Metallic Fuel Models of SAS4A using TREAT M-Series Overpower Test Simulations

A. Karahan[1], A. Tentner[1]

[1]Argonne National Laboratory (ANL), Argonne, Illinois, U.S.A.

E-mail: akarahan@anl.gov

Abstract. The SAS4A safety analysis code has been extended to include mechanistic and physics-based models of U-Pu-Zr and U-Zr metallic fuel pins. The simulation of various phenomena such as metal fuel component migration, fission gas behavior, clad wastage formation, gas swelling induced axial fuel expansion, in-pin and ex-pin molten fuel relocation, and clad failure models have been significantly enhanced. The integrated code is validated through analyses of eight metal fuel TREAT M-Series overpower experiments. In this study, the SAS4A calculated fuel reactivity and clad failure data are compared with the corresponding experimental data. The results show that the code satisfactorily predicts solid fuel axial expansion, molten fuel in-pin relocation, cladding loss due to rapid eutectic penetration, cladding creep fracture and molten fuel ejection to the coolant channel. The study shows that the uncertainties in transient response tend to be higher for the lower burnup fuel.

Key Words: metallic fuel models, severe accidents, TREAT overpower tests, SAS4A validation.

1. Introduction

Performing best estimate nuclear fuel performance analysis with physics-based approaches is critical in assessing the safety and performance of nuclear reactors. Combining individual models corresponding to essential phenomena could reduce the uncertainties of the predictions [1]. This approach provides also the way to compare the performance of different fuel types.

The SAS4A code was developed at Argonne National Laboratory for the system analysis and safety evaluation of liquid metal fast reactors [2]. Initially developed for the analysis of oxide fuel cores, the SAS4A capabilities were expanded to the analysis of U-Pu-Zr and U-Zr metal fuel cores. The code's metallic fuel performance models, in-pin fuel motion and post-failure fuel ejection models have recently been extended significantly [3-4], aiming for more mechanistic and comprehensive modelling of the essential metal fuel physical phenomena. New models cover the full range pre-transient characterization of the fuel, anticipated transients, design basis accidents and severe accident scenarios, valid up to loss of fuel assembly integrity. In this paper, the new metal fuel models are briefly introduced and the results of SAS4A validation analyses of several TREAT M-Series metal fuel experiments are presented. The benchmarking effort focused on the calculation of fuel reactivity changes and the fuel pin failure observed during tests.

2. Metallic Fuel Models in SAS4A

The metal fuel performance models for the pre-transient characterization and transient analysis are called SSCOMP-A and DEFORM-5A, respectively. DEFORM-5A covers the fuel behavior prior to the fuel pin cladding failure and post-failure fuel ejection. The in-pin molten fuel motion prior to fuel pin failure is modeled by PINACLE-M. The post-failure metal fuel ejection into the coolant channel and subsequent fuel relocation is modeled by LEVITATE-M. The description of these models can also be found in a companion paper presented at this conference [4].

2.1. SSCOMP-A and DEFORM-5A

The main components of SSCOMP-A and DEFORM-5A are (1) fuel pin mechanical analysis, (2) fuel swelling and fission gas behavior, (3) fuel clad chemical interaction, (4) fuel constituent redistribution, (5) clad failure, (6) sodium infiltration into the fuel slug, (7) dynamic computation of burnup dependent evolution of nuclide groups, U-235, U-238, Pu-239, Pu-240, Pu-241, Pu-242, Minor Actinides, Lanthanides, fission gas, Zirconium, and other fission products, and corresponding reactivity feedback coefficients of each nuclide groups. The total computation time requirement for the pre-transient characterization of the EBR-II high burnup fuel and transient simulation of the TREAT case with SSCOMP-A and DEFORM-5A is about six minutes with a regular PC.

SSCOMP-A module simulates the evolution during irradiation of essential fuel pin parameters such as fuel swelling, fission gas release, fuel axial elongation, fuel constituent redistribution, iron diffusion to the fuel surface, clad wastage formation due to lanthanide attack, clad straining, and clad failure margin, satisfactorily. It is validated using EBR-II normal operation database up to 19 at % [5-7].

DEFORM-5A is the transient fuel performance model. The model is an extension of SSCOMP-A, while addressing the issues such as rapid changing conditions during the transient, eutectic formation between the fuel and cladding, gas bubble behavior, creep of the soft fuel and clad failure. Above the eutectic formation temperature, the fuel mechanical analysis model computes the axial relocation of the frictionless and soft solid fuel. The fission gas model tracks the non-equilibrium gas bubble behavior and formation of large bubbles at elevated temperatures. The eutectic formation model tracks for the iron dissolution, actinide migration, and penetration of the liquefied region towards the cladding. The clad failure models include a CDF based empirical model and a mechanistic clad failure model based on tracking of the grain boundary cavities driven by creep and diffusion.

2.2. PINACLE-M and LEVITATE-M

The PINACLE-M module describes the in-pin molten metal fuel relocation prior to cladding failure. It is an Eulerian, two-phase, transient hydrodynamic model based on solution of 1D mass, momentum and energy equations, describing in-pin axial fuel relocation in the variable-area pin cavity. PINACLE-M tracks the relocation of each of the melting U-Zr and U-Pu-Zr metal fuel components, including the nuclide groups tracked by SSCOMP-A. The local fuel composition is a function of burnup and associated fuel composition changes. PINACLE-M is activated upon fuel melting and formation of the molten fuel cavity. The axial relocation of the molten fuel in the cavity is driven by the growth of the fission gas bubbles and sodium evaporation. In-pin molten fuel motion is one of the most important features of the metallic fuel. Axial relocation of the molten fuel combined with the expansion of the soft solid fuel could bring enough negative reactivity to naturally shutdown the reactor.

The LEVITATE-M module describes the post-failure fuel ejection into the coolant channel and the thermal-hydraulics behavior of the multi-component and multi-phase flow in the coolant channel upon fuel ejection. After the occurrence of cladding failure LEVITATE-M describes the axial fuel relocation of the fuel ejected in the coolant channel and continues to describe the in-pin fuel relocation previously described by PINACLE-M.

3. TREAT M-Series Tests

TREAT M-Series transient overpower (TOP) metal fuel test results [8-9] were used to benchmark the SAS4A metal fuel models. The tests were performed between 1984 and 1987 in Transient Reactor Test Facility (TREAT) in Idaho Falls, ID. The purpose of the tests was to (1) determine the cladding failure time or margin, (2) assess the fuel reactivity changes due to pre-failure in-pin axial expansion, and (3) assess the post-failure events upon cladding failure.

3.1. Description of the Test Fuel

The TREAT test metal fuel pins were irradiated in EBR-II. The test metal fuel pins have 72.5 % smear density and plenum to fuel ratio is unity. The peak linear heat rate and burnup varies between 35 - 45 kW/m and 0 - 10 at %, respectively. Most fuel pins consist of U-19Pu-10Zr fuel slugs and use D9 type cladding materials. Only one fuel pin has U-10Zr fuel slug and HT9 cladding material.

The pre-transient characterization of the test fuel was performed by the SSCOMP-A model of SAS4A using the real irradiation history of the corresponding fuel pins. The parameters such as fuel constituent redistribution, porosity evolution, fission gas release and plenum pressurization, cladding wastage, clad straining, fuel axial elongation were predicted and recorded prior to the transient.

3.2. Description of the Transient Overpower Scenario

FIG. 1 shows the Mark-III integral sodium loop and a typical transient power history for the M-series tests. The tests assumed a set of reference operating conditions. Then the power is increased with respect to the nominal value. The nominal conditions are 40 kW/m peak linear heat rate, 630 K inlet coolant temperature and 150 K coolant temperature rise. The axial power shape is chopped cosine. The radial power distribution was affected by thermal neutron flux depression and the constituent redistribution of the actinides. During the transient the power was increased to three to five times with respect to its nominal value in approximately eight seconds. Table I shows the eight test cases and the corresponding maximum power levels during the transient. Reactor shutdown took place if the prescribed power level was reached or fuel failure occurred.

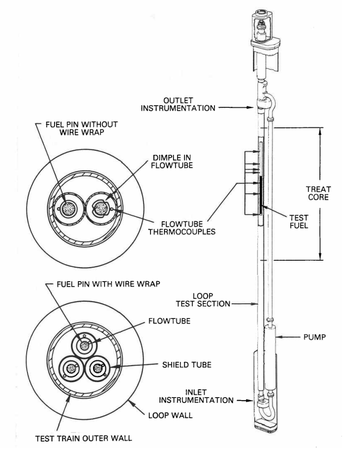

FIG. 1(a) Mark-III integral sodium loop

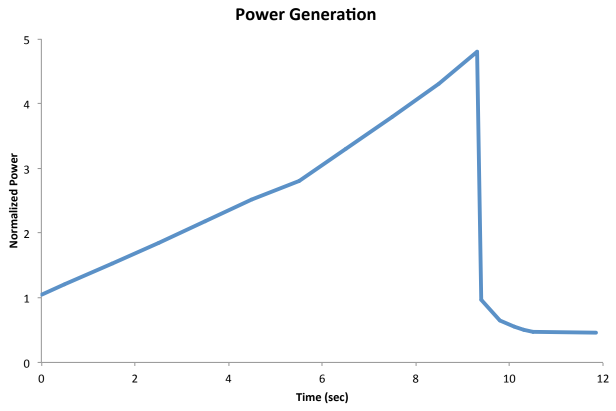

FIG. 1(b) M7 Test U-10Zr/HT9 Burnup=2.9 at %.

4. Benchmark Results and Discussion

4.1. Fuel Failure Benchmarks

Failure margin predictions and the test results are compared in Table I. The results indicate that power ratio of 4.3 is roughly critical point for the onset of rapid eutectic penetration for U-19Pu-10Zr fuel pins. At power ratio of 4.4, significant eutectic penetration occurs for M6-53 test pin. M7-29 fuel pin, which is U-10Zr fuel slug, operated at power ratio 4.8, much higher than M6-53, and did not fail. The reason is due to lower rate of rapid eutectic penetration of U-10Zr fuel alloys compared to U-19Pu-10Zr fuel alloys. M7-98 test pin failed without any significant eutectic penetration because the power ratio was low compared to previous cases. Combination of high burnup and low plenum to fuel volume ratio, resulted in operating with high plenum pressure and high cladding irradiation dose. As a consequence, plenum pressure induced creep rupture has occurred for this case. Table I shows that the new fuel models of SAS4A satisfactorily predict the rapid eutectic penetration and creep induced clad failure behavior.

TABLE I: TREAT-M Series Test Results.

Test No.	Fuel Pin Material	Peak Burnup (at %)	Power to Flow Ratio	Clad Wastage (μm)	Clad Failure-Experiment	Clad Failure-Simulation CDF/Failure Time
M5-08-F1	U-19Pu-10Zr	0.8	3.4	3	No Failure	No Failure CDF=0.7E-05
M5-19-F1	U-19Pu-10Zr	1.9	3.4	6	No Failure	No Failure CDF=1.8E-05
M5-08-F2	U-19Pu-10Zr	0.8	4.3	166	No Failure	No Failure CDF=3.6E-05
M5-19-F2	U-19Pu-10Zr	1.9	4.3	11	No Failure	No Failure CDF=6.3E-04
M6-19	U-19Pu-10Zr	1.9	4.4	149	No Failure	No Failure CDF=9.5E-04
M6-53	U-19Pu-10Zr	5.3	4.4	270	Failure at 13.23 s	Failure at 13.17 s
M7-29	U-10Zr	2.9	4.8	299	No Failure	No Failure CDF=0.2E-02
M7-98	U-19Pu-10Zr	9.8	4.0	42	Failure at 17.71 s	Failure at 17.67 s

4.2. Fuel Reactivity Worth Benchmarks

Measured and predicted relative fuel reactivity worth are compared for eight TREAT cases. Comparison given in Section-4.2.1 shows the behaviour prior to shutdown or fuel failure. Section-4.2.2 shows the effect of post-failure fuel ejection for the two failed fuel pins. In order to analyse the fuel relocation results, the fuel worth curves used in HODOSCOPE analysis of the experimental data are utilized. The relative fuel worth is calculated by dividing the integrated fuel reactivity worth at any given time by the integrated worth calculated at the reference conditions, when the fuel is still in the original configuration.

4.2.1. Reactivity Worth Prior to Fuel Failure

FIG. 2 through FIG. 8 shows the change in relative worth of the fuel due to axial relocation during the transient up to the time that fuel failure or reactor shutdown took place. Prior to fuel melting, the fission gas induced swelling, thermal expansion, and fuel creep plays an essential role for the fuel axial expansion. A large fraction of the pin length exceeded the eutectic formation temperature at the fuel-clad interface but only a small fraction of the pin length has reached the rapid eutectic penetration regime. Upon the eutectic formation between the fuel and cladding, the friction between the fuel and cladding vanishes, promoting for the fuel axial expansion.

FIG. 2 shows the results for M5-F1-0.8 at % and M5-F1-1.9 at % cases, which are low burnup fuel pins. Furthermore, these tests targeted a relatively low power ratio, 3.4. As a result, a small reactivity change took place during the transient. No fuel melting or failure was observed. The comparison in FIG. 2 shows that SAS4A predictions match well with the experimental data.

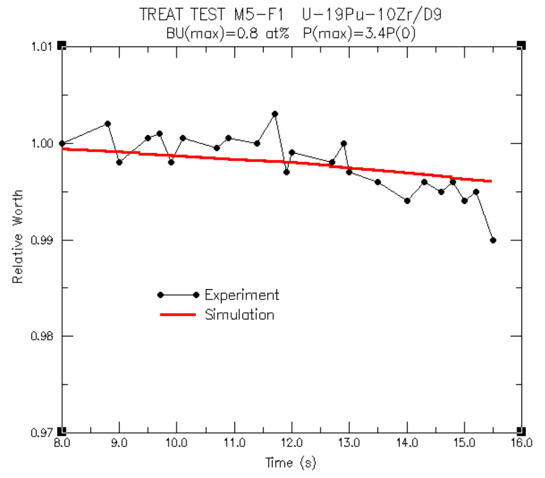

FIG. 2(a) Relative worth for M5-F1-0.8 at %

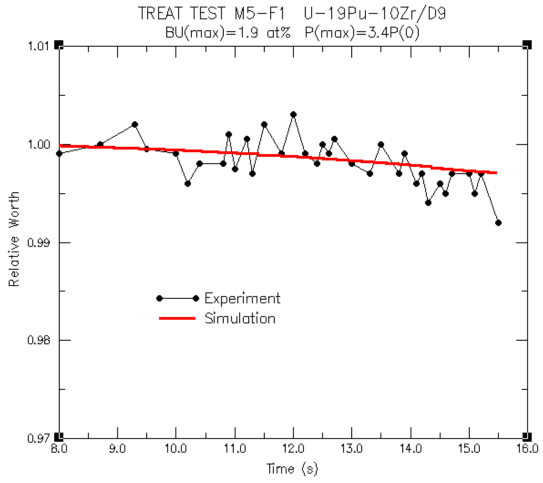

FIG. 2(b) Relative worth for M5-F1-1.9 at %

The comparison for M5-F2-0.8 at % case is shown in FIG. 3(a). This time, power ratio was 4.3. It is high enough melt the fuel. The progression of the central fuel cavity is shown in FIG. 3(b) by the red color region. The swelling of the low burnup fuel was not complete and the radial fuel relocation or compositional changes was minor prior to the transient. As a result, a central cavity forms. Moreover, sodium infiltration to the fuel did not take place due to low fuel porosity. The resulting in-pin molten fuel ejection remains small and predictions match well with the experimental data.

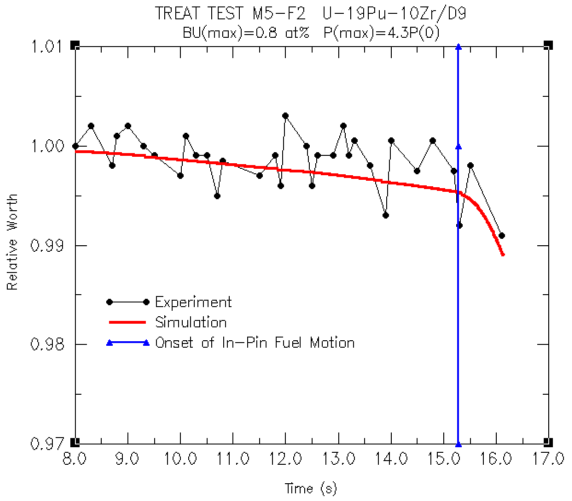

FIG. 3(a) Relative worth for M5-F2-0.8 at %

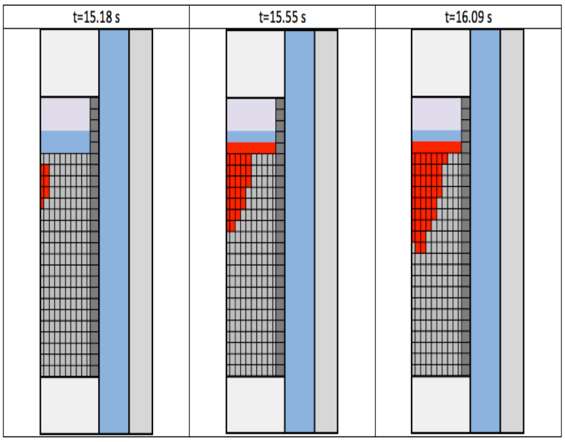

FIG. 3(b) Molten Cavity M5-F2-0.8 at %

FIG. 4(a) shows the fuel worth comparison for M5-F2-1.9 at % test. Power ratio is 4.3. Similar to other low burnup cases above, the fuel axial expansion prior to fuel melting remains small and the predictions match well with the experimental data. Upon melting, an annular molten fuel cavity (red color region) forms as shown in FIG. 4(b). Existence of the annular cavity is due to the radial relocation of the fuel constituents during normal operation. In addition, sodium infiltration was predicted for this test fuel during normal operation. During the transient, sodium evaporation took place at this low plenum pressure condition and promoted the fuel axial extrusion. Predicted reactivity change and fuel axial ejection for this case is higher than the experimental observations.

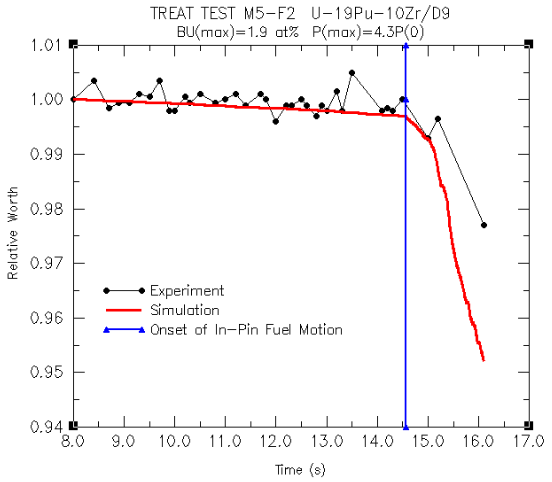

FIG. 4(a) Relative worth for M5-F2-1.9 at %

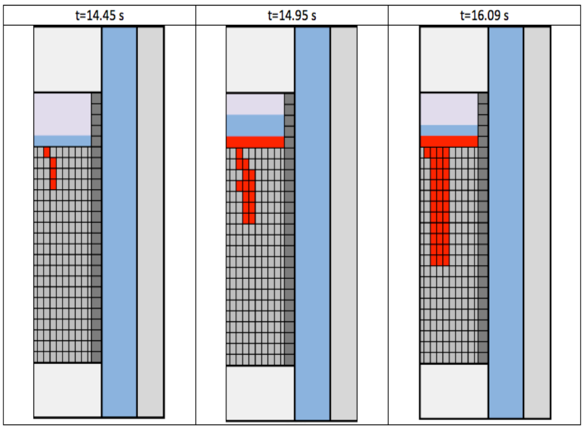

FIG. 4(b) Molten Cavity M5-F2-1.9 at %

FIG. 5(a) shows the fuel worth comparison for M6-1.9 at % test. Power ratio is 4.4. The test fuel pin bears very similar characteristics with the M5-F2-1.9 at %, considering burnup, pre-transient history, fuel composition and the transient scenario. As a result, SAS4A predictions for this fuel pin is very similar to the one predicted for M5-F2-1.9 at % fuel pin. However, as shown in FIG. 5(a), the match between the experimental data and the predicted relative fuel worth is satisfactory this time. Comparison of M5-F2-1.9 at % and M6-1.9 at % cases also reflect the uncertainties associated with low burnup fuel pin response. At low burnup, metallic fuel characteristics evolves rapidly. The fuel porosity, fuel constituent redistribution, swelling, fission gas release, sodium infiltration are progressive at low burnup and bear uncertainties. This may explain the observed differences between M5-F2-1.9 at % and M6-1.9 at % cases.

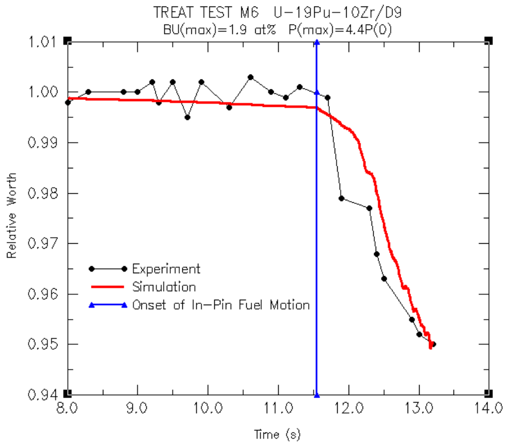

FIG. 5(a) Relative worth for M6-1.9 at %

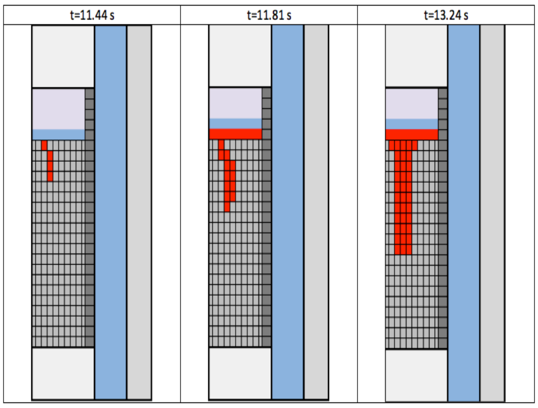

FIG. 5(b) Molten Cavity M6-1.9 at %

Fuel worth comparison for M6-5.3 at % test pin is shown in FIG. 6(a). The power ratio is 4.4. Medium burnup fuel was fully swollen during the pre-transient. Well-developed porosity structure and U/Zr radial redistribution took place during the normal operation. As a result of the fuel relocation, the fuel bears an annular region with low melting phases and the thermal resistance of the fuel is higher compared to low burnup cases. During the transient, magnitude of the predicted and measured solid fuel expansion is higher and match well with the measured data. It is due to aggravated or single direction axial expansion of the fully swollen and soft fuel. FIG. 6(b) depicts the molten fuel cavity and clad failure regions using red and yellow colors, respectively. Upon fuel melting, the molten fuel cavity formed is much larger than low burnup cases due to higher thermal resistance of the fuel. The molten fuel ejection enhances the relative worth change as shown in FIG. 6(a). However, the ejection is not as rapid or sharp as the low burnup cases due to absence of sodium evaporation. Higher plenum pressure for this test fuel pin did not allow for sodium evaporation. The fuel failure is predicted for this test fuel pin at top axial region, consistent with the experimental data.

FIG. 7(a) shows the relative fuel worth comparison for M7-2.9 at % test pin. The power ratio is 4.8, much higher than all other tests. Moreover, this is the only U-10Zr/HT9 fuel pin, as shown in Table I. The solid fuel axial expansion remains low, similar to other low burnup cases. It is also due to lower diffusivity, higher melting point and higher thermal conductivity characteristics of U-10Zr fuel compared to U-19Pu-10Zr fuel. FIG. 7(b) shows the progression of the molten cavity. Upon formation of the molten fuel cavity, the fuel axial ejection took place, mostly promoted by the sodium evaporation. The relative fuel worth predictions match well with the experimental observations.

FIG. 8(a) shows the relative fuel worth comparison for M7-9.8 at % test pin up to time at which fuel failure takes place. The power ratio is 4.0, lower than most cases discussed above. In contrast, the experimental data shows that change in relative worth is more significant compared to previous cases. In this case, the fuel thermal conductivity degradation is highest compared to other cases due to extensive fuel constituent redistribution of the high burnup fuel pin. As a result, a large cavity forms. Fuel ejection remains smooth due to absence of sodium evaporation. The predicted and observed relative worth changes and clad failure is satisfactory.

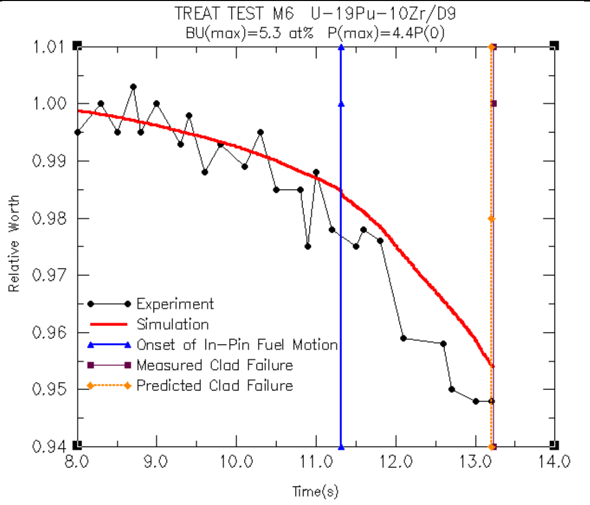

FIG. 6(a) Relative worth for M6-5.3 at %

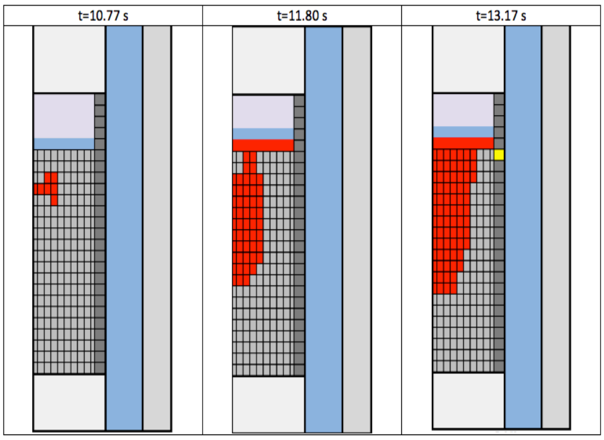

FIG. 6(b) Molten Cavity M6-5.3 at %

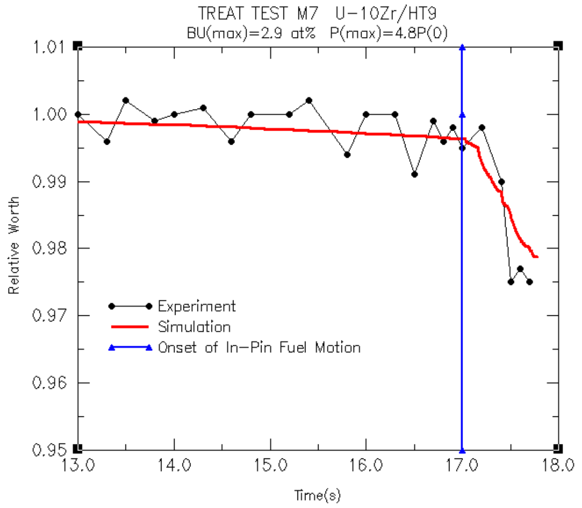

FIG. 7(a) Relative worth for M7-2.9 at %

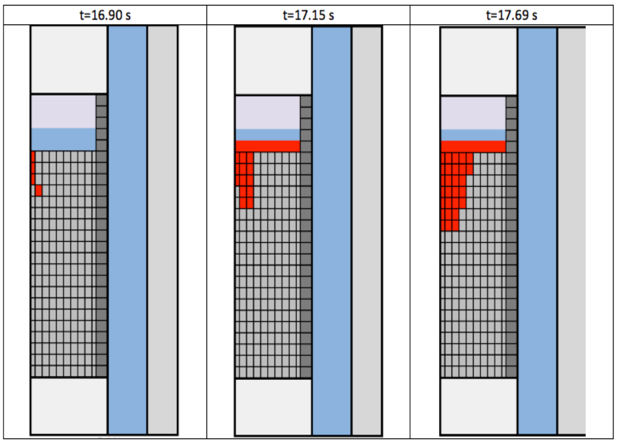

FIG. 7(b) Molten Cavity M7-2.9 at %

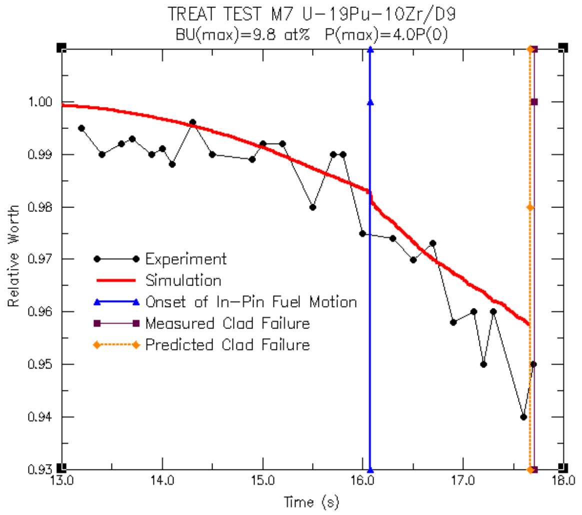

FIG. 8(a) Relative worth for M7-9.8 at %

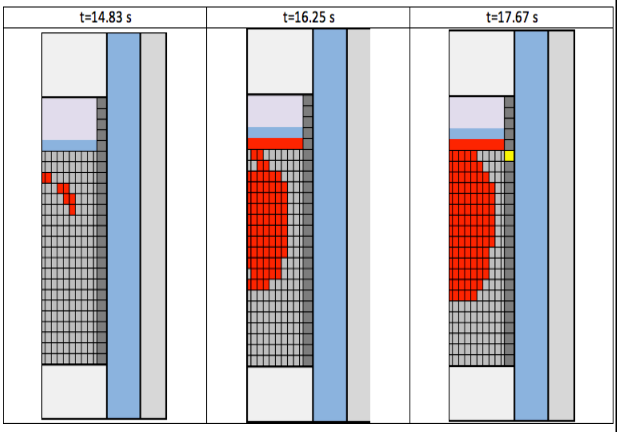

FIG. 8(b) Molten Cavity M7-9.8 at %

4.2.2. Post Failure Fuel Reactivity Benchmarks

FIG. 9 (a) and FIG. 9(b) show the pre-failure and post-failure relative fuel worth changes for M6-5.3 at % and M7-9.8 at % cases, respectively. Upon fuel failure at the top axial location, the fuel ejection took place under the pressure difference between the fuel pin cavity and the coolant channel. The initial in-pin fuel relocation accelerates the fuel towards the failure location, leading to a negative worth contribution. The discharged molten fuel leads to an increase in fuel channel pressure, which acts to disperse the fuel away from the failure location. Because the coolant pump remains ON after fuel failure, the discharged fuel is relocated mostly upward and out of the active fuel region. The SAS4A simulation was terminated when in-pin fuel freezing took place. FIG. 9(a) shows that the predicted and measured post-failure relative worth for M6-5.3 at % test pin matches satisfactorily. The comparison given for M7-9.8 at % case in FIG. 9(b) shows that the predicted fuel ejection is faster and somewhat overestimated compared to the experimental measurements. Considering that there are uncertainties associated with the fuel flow dynamics the post-failure fuel ejection predictions match reasonably well with the experimental measurements. It is noted that the LEVITATE-M model has only recently become available, and further model enhancements and evaluation of the existing models are planned.

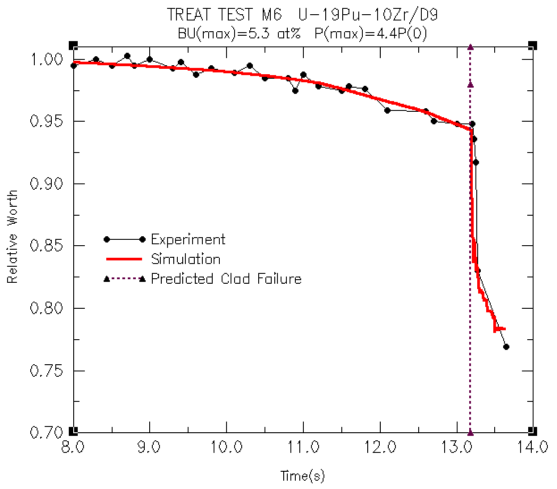

FIG. 9(a) Relative worth for M6-5.3 at %

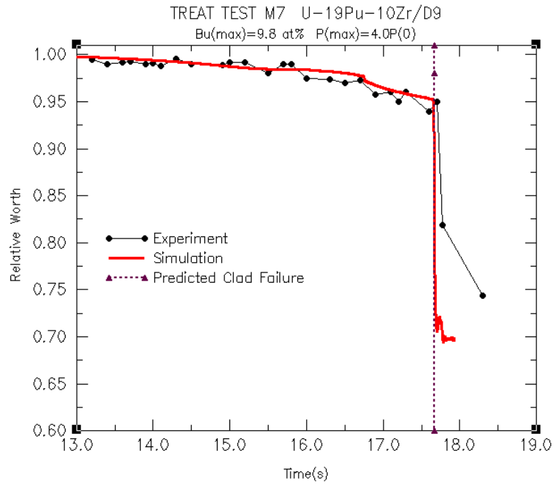

FIG. 9(b) Relative worth for M7-9.8 at %

5. Conclusions

In this study, the validation of the SAS4A safety analysis code using the new metallic fuel models was accomplished using TREAT M-Series transient overpower test cases including post-failure fuel ejection and up to the in-pin fuel freezing. The results indicate that the mechanistic and physics-based metal fuel models capture the sensitivity to various conditions related to pre-transient operation and transient conditions. Considering the fact that there are several fuel performance and flow dynamics related sources of uncertainties associated with the pre-transient characterization of the fuel as well as in-pin molten fuel motion and post-failure fuel ejection, comparisons of measured data and SAS4A predictions of fuel worth evolution and cladding failure are found to be satisfactory.

ACKNOWLEDGEMENTS

This work is performed in the framework of collaboration between Argonne National Laboratory and the Korea Atomic Energy Research Institute under interagency agreement, through U.S. Department of Energy contract DE-AC02-06CH11357.

REFERENCES

[1] KARAHAN, A., KAZIMI, M. S., “On the Significance of Modeling Nuclear Fuel Behavior with Right Representation of Physical Phenomena”, Nuclear Engineering and Design, Vol. 241, 484-491, (2011).

[2] TENTNER, A., et al., “The SAS4A LMFBR Whole Core Accident Analysis Code”, Proceedings of International Topical Meeting on Fast Reactor Safety, Knoxville, TN, April, (1985).

[3] TENTNER A. M., KANG, S. H., KARAHAN, A., “SAS4A Metal Fuel Development for the Analysis of Postulated Severe Accidents in Metal Fuel Sodium Fast Reactors”, Transactions of American Nuclear Society, Las Vegas, NV, November, (2016).

[4] TENTNER A., KANG, S. H., KARAHAN, A., “Advanced in the Development of the SAS4A Code Metallic Fuel Models for the Analysis of PGSFR Postulated Severe Accidents,” International Conference on Fast Reactors and Related Fuel Cycles: Next Generation Nuclear Systems for Sustainable Development (FR-17), Yekaterinburg, Russian Federation, June, (2017).

[5] KARAHAN, A., “Development of Advanced In-Pin Metallic Fuel Performance Models for SAS4A”, Transactions of American Nuclear Society, Vol. 110, 912-915, June, (2014).

[6] KARAHAN, A., “Mechanistic Modeling of Metallic Fuel/Cladding Metallurgical Interactions”, Transactions of American Nuclear Society, Vol. 110, 747-750, June, (2014).

[7] KARAHAN, A., “Development of an Enhanced Mechanistic Model for Metallic Fuel Constituent Redistribution”, Transactions of American Nuclear Society, Vol. 110, 916-918, Vol. June, (2014).

[8] BAUER, T. H., Wright, A. E., ROBINSON, W. R., HOLLAND, J. W., RHODES, E. A., “Behavior of Modern Metallic Fuel in TREAT Transient Overpower Tests”, Nuclear Technology, 325-352, Vol. 92, (1990).

[9] RHODES, E. A., STANFORD, G. S., REGIS, J. P., BAUER, T. H., DICKERMAN, C. E., “Transient Feedback from Fuel Motion in Metal IFR Fuel,” Proceedings of International Topical Meeting on Fast Reactor Safety, Vol. 1, 453-462, Snowbird, Utah, August, (1990).